Electronic Supplementary Material (ESI) for Journal of Materials Chemistry A.

Screw-like PdPt nanowires as highly efficient electrocatalysts for methanol and ethylene glycol oxidation

Jing-Xiao Tang,[a] Qing-Song Chen,*[a] Le-Xing You,[c] Hong-Gang Liao,[b] Shi-Gang Sun,*[b] Shun-Gui Zhou,[c] Zhong-Ning Xu,[a] Yu-Min Chen,[a] Guo-Cong Guo*[a]

a. State Key Laboratory of Structural Chemistry, Fujian Institute of Research on the Structure of Matter, Chinese Academy of Sciences, Fuzhou, Fujian 350002, P. R. China.

b. State Key Laboratory of Physical Chemistry of Solid Surfaces, Department of Chemistry, College of Chemistry and Chemical Engineering, Xiamen University, Xiamen, 361005, P. R. China.

c. Fujian Provincial Key Laboratory of Soil Environmental Health and Regulation, College of Resources and Environment, Fujian Agriculture and Forestry University, ShangXiaDian Road 15, Fuzhou, 350002, P. R. China.

*Email: gcguo@fjirsm.ac.cn (G.-C. Guo); chenqs@fjirsm.ac.cn (Q.-S. Chen); sgsun@xmu.edu.cn (S.-G. Sun)

1. Chemicals and materials

The glassy-carbon electrode (99.99%, Φ = 3 mm) was purchased from Takai Carbon Co., LTD. (Tokyo, Japan). Commercial Pd/C (20 wt.%), Pt/C (20 wt.%) and Nafion (5% w/w solution) were purchased from Alfa Aesar (Tianjin, China). NaOH, methanol, ethylene glycol and $PdCl_2$ were purchased from Sinopharm Chemical Reagent Co., LTD. (Shanghai, China). K_2PtCl_6 was purchased from Adamas-Reagent Co., LTD. (Shanghai, China). Sulfuric acid (EMSURE® ACS) was purchased from Merck. Argon (99.999%) and CO (99.99%) were purchased from Xinhang gas Co., LTD (Fuzhou). All the chemicals were used as received without further purification. The ultra-pure water (18 MΩ cm) for cleaning glassware and solution preparation was produced from the Millipore system.

2. The schemes of square-wave potential program applied for preparation of PdPt NWs and Pt THHs

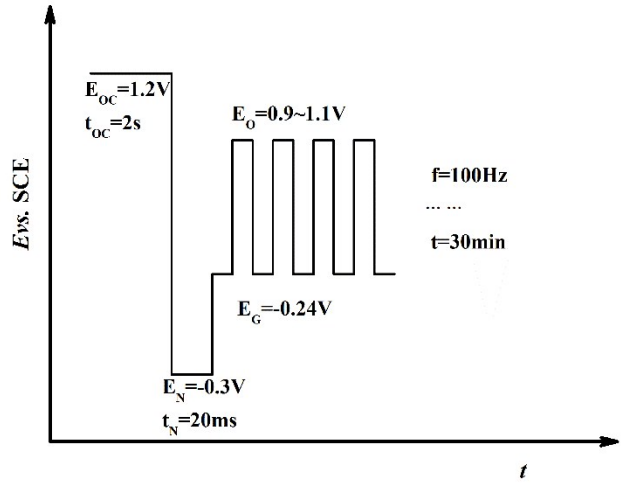

Fig. S1 Scheme of pulse waveform applied for preparation of PdPt NWs.

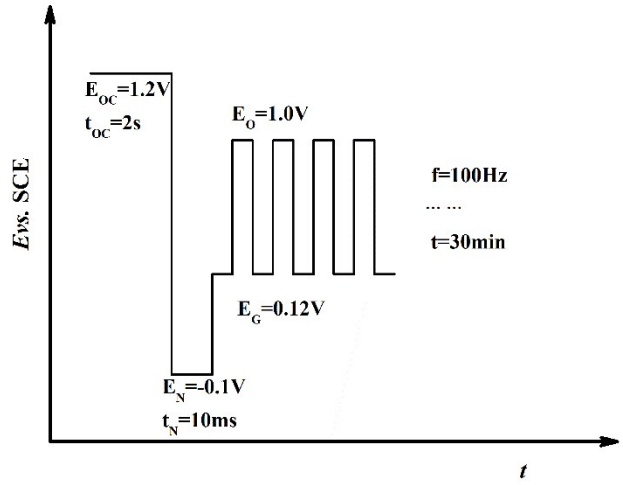

Fig. S2 Scheme of pulse waveform applied for preparation of THH Pt NCs.

3. Influences of electrodeposition conditions on the PdPt nanostructure

The formation of the unique structure of PdPt NWs was affected by several factors. Firstly, the applied potentials are important parameters to control the synthesis of PdPt NWs. In order to obtain PdPt NWs, the potential step region (from -0.24 to 0.9, 1.0, 1.1 V) used in the SWP procedure was wider than that for PdPt THHs (from 0.3 to 0.7 V) as reported in elsewhere.[1] This suggests that a higher growth rate of Pd, Pt and deeper surface oxygen adsorption is required to prepare PdPt NWs.[2] On the other hand, the variation of step potential could also affect the ratio of Pd:Pt in the alloys as mentioned in this paper. Secondly, the ratio of Pd^{2+} and Pt^{4+} in the precursor solution could also affect the shape and composition of PdPt alloys. For example, when the potential step region was fixed at -0.24 ~ 1 V and the deposition solution only content Pd^{2+} or Pt^{4+}, Pd tends to grow into irregular branch like nanostructure, Pt tends to grow into aggregated irregular nanoparticle (see Fig. S3a and d). In Pd^{2+} and Pt^{4+} containing solution, when the content of Pd^{2+} in the precursor solution is lower than 50% or higher than 90%, PdPt NWs could not be achieved successfully (see Fig. S3b and c). Finally, the deposition time is also important to prepare the perfect PdPt NWs. The growing process of PdPt was monitored by SEM with varying growth time (see details in Fig. S4). At the initial nucleation stage, the PdPt nuclei could not be observed clearly except

some bigger nanoparticles limited by the resolution of SEM. After 5 min of growth, a few PdPt nanowires with much branches appeared. With the growth time increasing, part of the small branches may be dissolved at the high oxidation potential step, and part of them grew longer. And after 30 min, the electrode surface was covered by well-defined PdPt screw thread like nanowire networks.

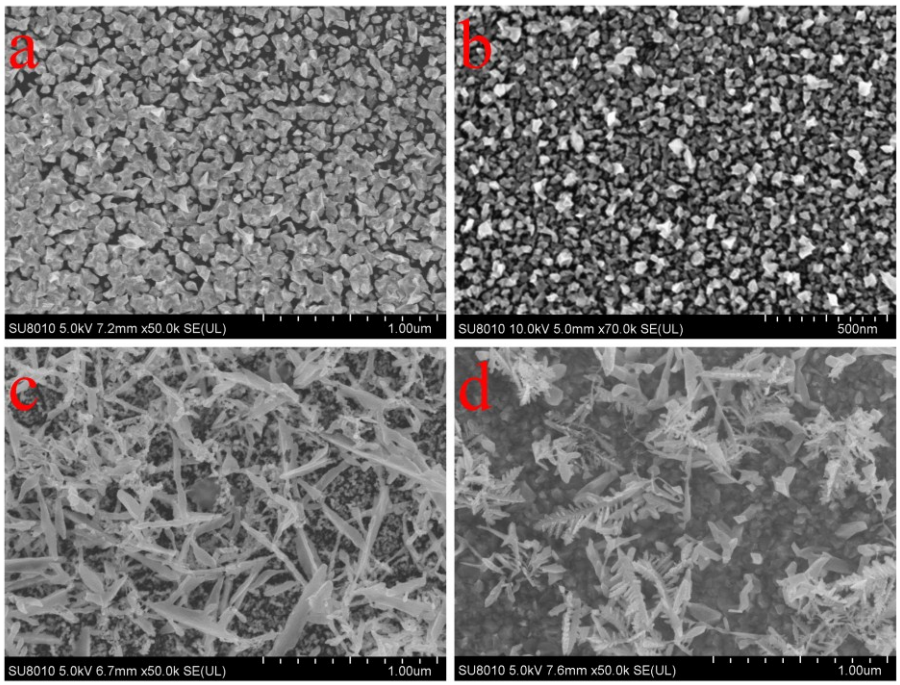

Fig. S3 SEM images of catalysts synthesized from different precursor solutions. (a) 1.5 mM K_2PtCl_6 + 0.1 M H_2SO_4; (b) 1.2 mM K_2PtCl_6 + 0.3 mM H_2PdCl_4 + 0.1 M H_2SO_4; (c) 0.15 mM K_2PtCl_6 + 1.35 mM H_2PdCl_4 + 0.1 M H_2SO_4; (d) 1.5 mM H_2PdCl_4 + 0.1 M H_2SO_4. Electrochemical deposition parameters are the same to that used for PdPt NWs.

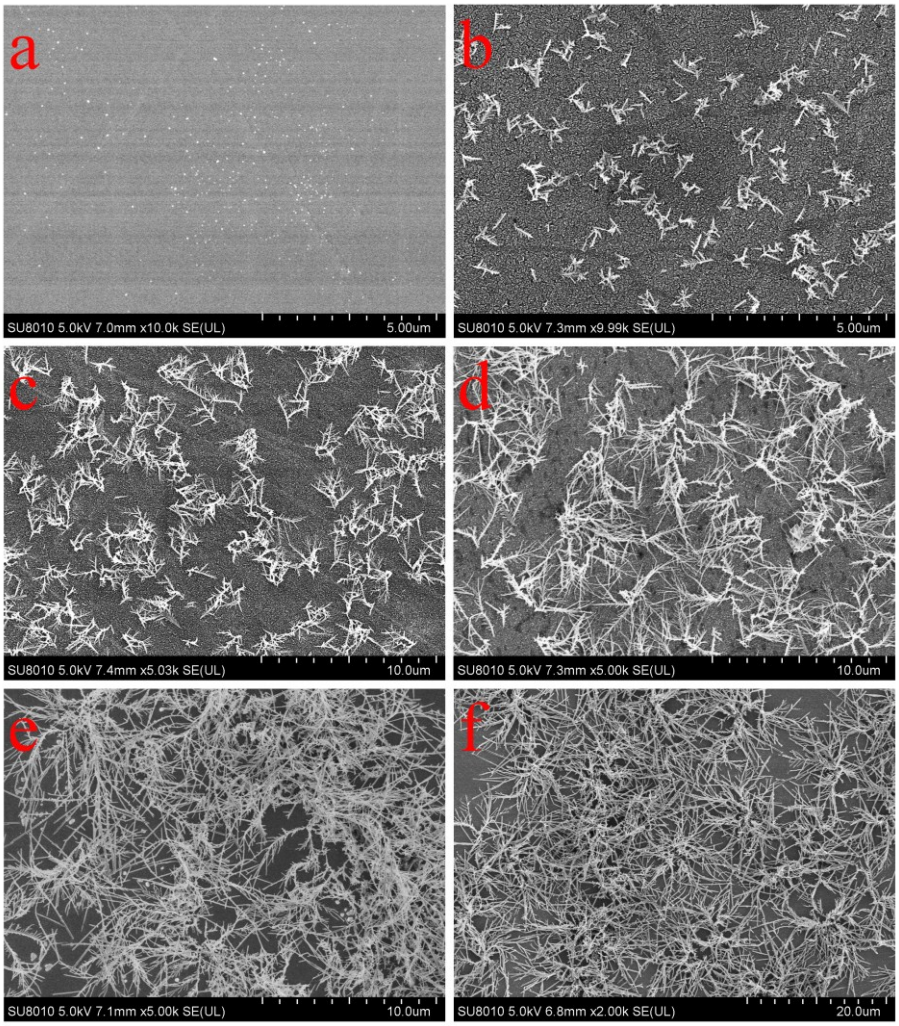

Fig. S4 SEM images of PdPt NWs catalysts with different growth time. (a) nucleation stage; (b) 5 min; (c) 10 min; (d) 20 min; (e) 30 min; (f) 60 min.

4. EDS analysis of PdPt NWs

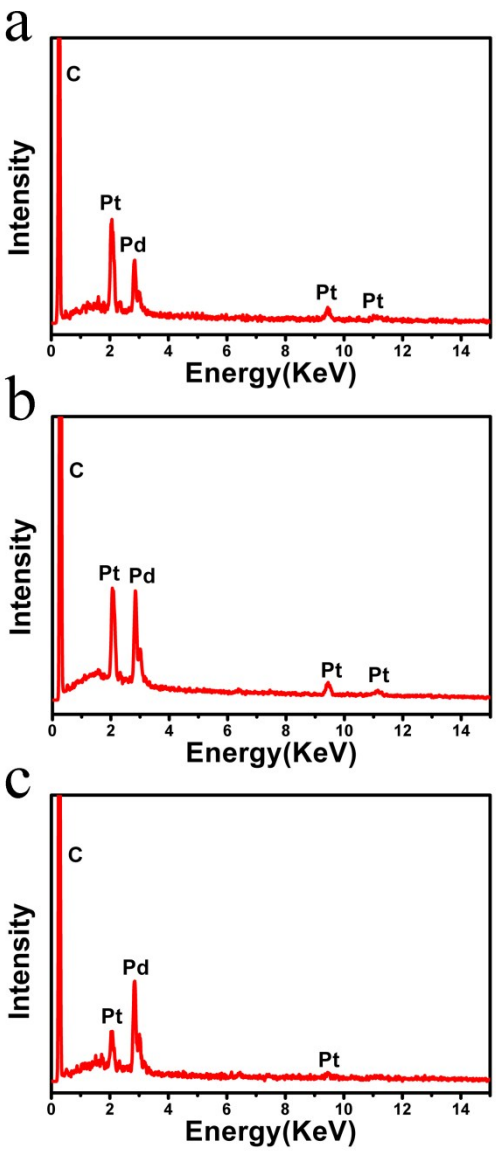

Fig. S5 EDS spectrum of PdPt NWs catalysts. (a) Pd_1Pt_1 NWs; (b) Pd_2Pt_1 NWs; (c) Pd_3Pt_1 NWs.

5. Atomic model of {hk0} and {hkk} facets

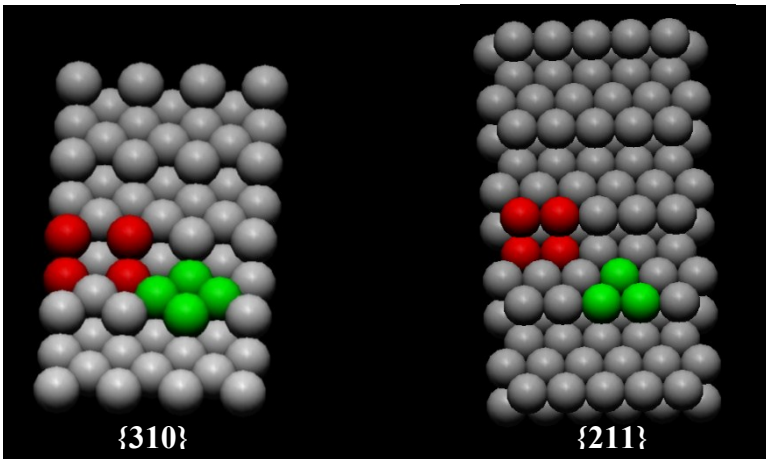

Fig. S6 Atomic model of {310} and {211} as representative of {hk0} and {hkk} facets, respectively.

6. Comparison of TRFTIR spectra of EGOR on Pd_1Pt_1 NWs and Pt THHs

TRFTIR spectra of EG oxidation on Pd_1Pt_1 NWs and Pt THHs are shown in Fig. S5 recorded successively at different reaction time (t) with E_R = -0.75 V and E_S = 0 V in 0.5 M EG + 0.5 M NaOH solution. The acquisition time was approximately 8.6 s per spectrum. However, to simplify the figure, the spectra with an interval of 17.2 s are displayed in Fig. S5. With the increase of t, different variation trends can be clearly observed for EGOR on Pd_1Pt_1 NWs and Pt THHs. The most obvious differences involve in the bands related to CO_2, HCO_3^- and oxalate species.

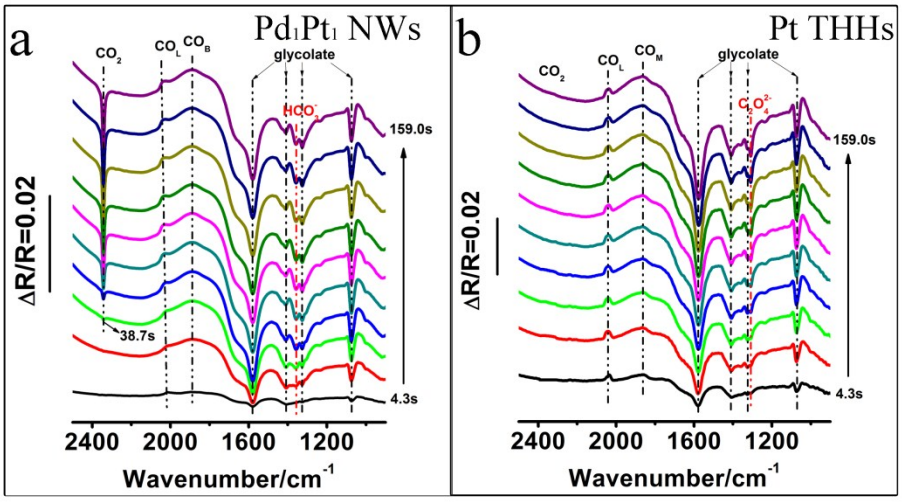

Fig. S7 TRFTIR Spectra of Pd_1Pt_1 NSNWs (a) and Pt THHs (b) in 0.5 M EG + 0.5 M NaOH solution, E_S = 0 V, E_R = -0.75 V.

7. Estimation of mass activity of Pd_1Pt_1 NWs

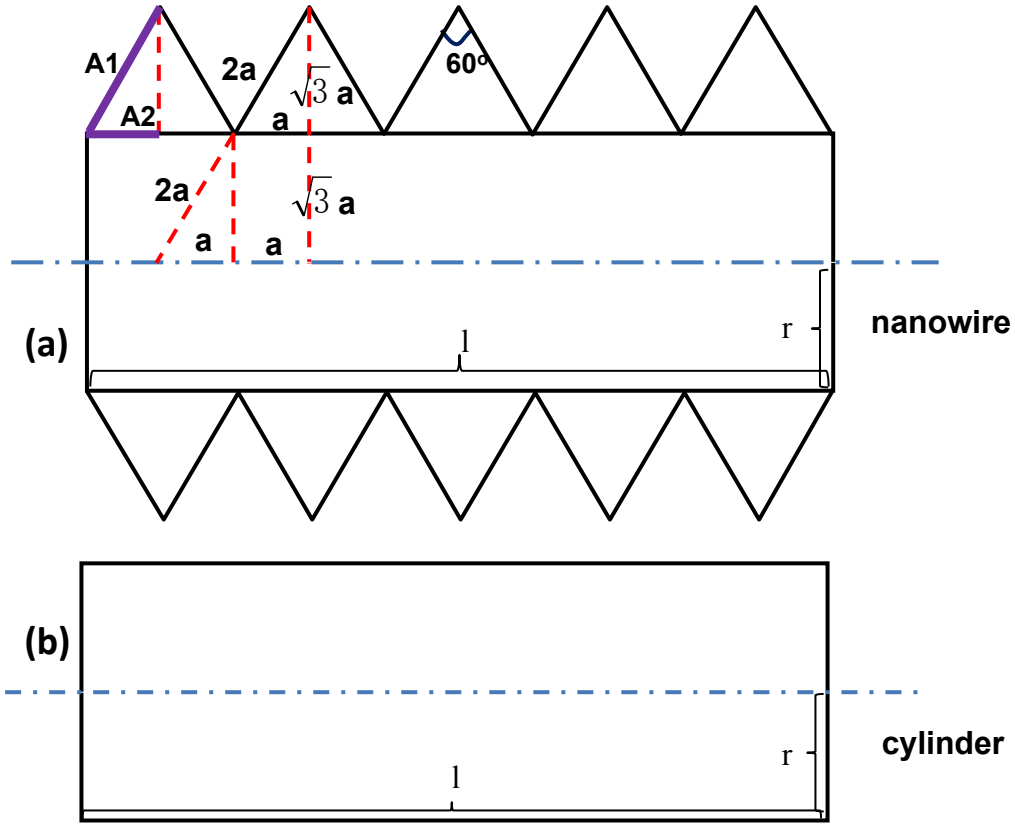

Fig. S8 A zigzag cylinder model for nanowire (a) and the smooth cylinder model (b).

The screw-like Pd_1Pt_1 NWs could be roughly simplified as the above zigzag model, its surface area and volume is compared to those of the corresponding cylinder model and has the ratio as follows:

① $A_{NW} / A_{cl} = A_1 / A_2 = (\pi \times 2\sqrt{3}\,a \times 4a - \pi \times \sqrt{3}\,a \times 2a) / (2\pi \times \sqrt{3}\,a \times a) = 3$

② $V_{NW} / V_{cl} = ((\pi \times (2\sqrt{3}\,a)^2 \times 2a) / 3 - (\pi \times (\sqrt{3}\,a)^2 \times a) / 3) / (\pi \times (\sqrt{3}\,a)^2 \times a)) = 7/3$

The mass specific surface area can be calculated as follows:

③ $S_{cl} = A_{cl} / m_{cl} = A / (V\rho) = 2\pi rl / (\pi r^2 l\rho) = 2 / (r\rho) = 15.94\ m^2/g$ (the average diameter of PdPt NWs is ca. 30 nm, r = 7.5 nm, $\rho = 16.73\ g/cm^3$)

④ $S_{NW} = S_{cl} \times (A_{NW} / m_{NW}) / (A_{cl} / m_{cl}) = S_{cl} \times (A_{NW} / A_{cl}) \times (V_{cl} / V_{NW}) = 15.94 \times 3 \times 3 / 7 = 20.49\ m^2/g$

The Pt THHs could be simplified as a spherical model,[3] thus the mass specific surface

area can be calculated as follows:

δ $S_{Pt,THHs} = A / m = A / (V\rho) = 4\pi r^2 / ((4/3)\pi r^3 \rho) = 3 / (r\rho) = 0.69\ m^2/g$ (the average size of THHs is ca. 500 nm, r = 250 nm, $\rho = 21.45\ g/cm^3$)

According to the area specific activity (j_f) in the forward scan, the mass activity ($j_m = j_f \times S_{NW}$) of Pd_1Pt_1 NWs for MOR and EGOR were estimated to be 2604 and 3469 A/g, respectively. The mass activity is about 2.9 and 1.9 times higher than that of MOR (889A/g) and EGOR (1821 A/g) on Pt/C, respectively. Because of the relative large diameter of Pt THHs, the mass activity of Pt THHs is much lower for MOR (35.8 A/g) and EGOR (110.7 A/g).

8. Supplementary tables

Table S1 Atomic ratio of Pd and Pt acquired respectively from EDS and XPS analysis of various catalysts; Onset and peak potential of CO stripping and ECSA of different catalysts for MOR and EGOR.

Catalyst	$(Pd:Pt)_{EDS}$	$(Pd:Pt)_{XPS}$	E_{onset} / V	$E_{p,CO}$ / V	ECSA/ cm^2, MOR	ECSA/ cm^2, EGOR
Pd_1Pt_1	50.3:49.7	41.4:58.6	-0.58	-0.27	0.37	0.32
Pd_2Pt_1	66.2:33.8	58.3:41.7	-0.58	-0.26	0.64	0.56
Pd_3Pt_1	75.4:24.6	60.5:39.5	-0.56	-0.25	0.68	0.68
Pt THHs	0:1	0:1	-0.55	-0.37, -0.33	0.15	0.15
Pt/C	0:1	0:1	-0.55	-0.30, -0.18	1.52	1.16
Pd/C	1:0	1:0	-0.47	-0.19, -0.14	0.42	0.34

Table S2 Binding energy (BE) and relative intensity obtained from Pd 3d XPS spectra of different catalysts.

	Pd_1Pt_1		Pd_2Pt_1		Pd_3Pt_1		Pd/C	
Species	B.E. (eV)	Relative intensity (%)	B.E. (eV)	Relative intensity (%)	B.E. (eV)	Relative intensity (%)	B.E. (eV)	Relative intensity (%)
Pd(0)	335. 8	36.6	335.9	39.4	336.0	40.0	335.4	46.7
$Pd(OH)_x$	336.3	17.5	336. 5	17.0	336.5	25.0	336.0	27.8
PdO	336.9	36.9	337.1	36.3	337.1	20.2	336.8	13.1
PdO_2	338.2	9.0	338.6	7.3	338.0	14.8	338.5	12.4

Table S3 Binding energy (BE) and relative intensity obtained from Pt 4f XPS spectra of different catalysts.

	Pd_1Pt_1		Pd_2Pt_1		Pd_3Pt_1		Pt THHs		Pt/C	
Species	B.E. (eV)	Relative intensity (%)	B.E. (eV)	Relative intensity (%)	B.E. (eV)	Relative intensity (%)	B.E. (eV)	Relative intensity (%)	B.E. (eV)	Relative intensity (%)
Pt(0)	71.5	39.1	71.6	46.2	71.7	47.0	71.4	40.7	71.5	50.7
Pt(II)	72.1	46.0	72.3	40.4	72.4	34.2	72.0	46.3	72.4	34.2
Pt(IV)	73.5	14.9	73.7	13.4	73.6	18.8	73.3	13.0	73.7	15.1

Table S4 Comparison of catalytic performance for MOR and EGOR on different catalysts.

	MOR						EGOR					
Catalyst	E_{onset}	E_{pf}	j_f	q_f	q_b	q_f/q_b	E_{onset}	E_{pf}	j_f	q_f	q_b	q_f/q_b
Pd_1Pt_1	-0.56	-0.17	12.71	1.88	1.03	1.83	-0.52	-0.08	16.93	5.07	1.98	2.56
Pd_2Pt_1	-0.52	-0.14	10.01	1.44	0.68	2.12	-0.52	-0.03	15.22	4.50	1.40	3.21
Pd_3Pt_1	-0.52	-0.14	9.91	1.13	0.51	2.22	-0.52	-0.002	14.36	3.92	0.97	4.04
Pt THHs	-0.53	-0.25	5.19	0.78	0.63	1.24	-0.52	-0.19	16.05	2.66	1.28	2.08
Pt/C	-0.53	-0.15	2.33	0.49	0.25	1.96	-0.51	-0.06	6.28	1.77	0.79	2.24
Pd/C	-0.43	-0.19	0.91	0.16	0.09	1.78	-0.47	-0.15	4.18	0.67	0.30	2.23

E_{onset} (V): onset potential; E_{pf} (V), j_f (mA cm^{-2}) and q_f (mC cm^{-2}): the peak potential, peak current density and coulombic charge in the forward scan; q_b (mC cm^{-2}): coulombic charge in the backward scan; q_f/q_b: the ratio of forward and backward coulombic charges.

Table S5 MOR activities of various catalysts.

Catalysts	Electrolyte	Scan rate / mV s^{-1}	j_f / mA cm^{-2}	Ref.
Pd_1Pt_1	0.5 M CH_3OH + 0.5 M NaOH	50	12.71	This work
Pd_2Pt_1	0.5 M CH_3OH + 0.5 M NaOH	50	10.01	This work
Pd_3Pt_1	0.5 M CH_3OH + 0.5 M NaOH	50	9.91	This work
Pt THHs	0.5 M CH_3OH + 0.5 M NaOH	50	5.19	This work
$PtCu_{2.1}$ NWs	0.2 M CH_3OH + 0.1 M $HClO_4$	50	3.31	4
Pt_3Co NWs	0.2 M CH_3OH + 0.1 M $HClO_4$	50	1.95	5
Co@Pt	0.1 M CH_3OH + 0.1 M NaOH	50	1.79	6
PdPt nanodendrites	1.0 M CH_3OH + 1.0 M KOH	50	3.34	7
$Pd_{16}Pt_{84}$	0.1 M CH_3OH + 0.1 M $HClO_4$		1.96	8
Co_5Pt_{95}	0.1 M CH_3OH + 0.1 M $HClO_4$		1.6	8
$Pd_{34}Pt_{66}$	0.1 M CH_3OH + 0.1 M $HClO_4$	50	0.7	9
$Pd_{47}Pt_{53}$ NCs	1M CH_3OH + 0.1 M $HClO_4$	50	1.49	10
Porous Pt NTs	1M CH_3OH + 0.5 M H_2SO_4		1.62	11

j_f: specific activity.

Table S6 EGOR activities of various catalysts.

Catalysts	Electrolyte	Scan rate / mV s^{-1}	j_f / mA cm^{-2}	Ref.
Pd_1Pt_1	0.5 M EG + 0.5 M NaOH	50	16.93	This work
Pd_2Pt_1	0.5 M EG + 0.5 M NaOH	50	15.22	This work
Pd_3Pt_1	0.5 M EG + 0.5 M NaOH	50	14.36	This work
Pt THHs	0.5 M EG + 0.5 M NaOH	50	16.05	This work
$Pd_{55}Pt_{30}$	0.5M EG + 0.5M KOH	50	15.22	12
$Pd_{62}Au_{21}Ni_{17}$	0.5M EG + 0.5M KOH.	50	12/7	13
PdPt nanodendrites	1.0M EG + 1.0M KOH	50	5.2	7
PdPt multipods	1.0 M EG + 1.0 M KOH	50	8.42	14
PtPdCo nanoflowers	0.5 M EG + 1.0 M KOH	50	7.22	15
PtPd@Pt NCs/rGO)	0.5 M EG + 0.5 M H_2SO_4	50	1.87	16
$Pt_{84}Ru_{16}$	0.1M EG + 1.0M KOH	10	2.11	17
$Pt_{96}Sn_4$	0.1M EG + 1.0M KOH	10	1.41	17

j_f: specific activity.

Table S7 IR bands and their assignment appeared in the IR spectra of MOR and EGOR on Pd_1Pt_1 NSNWs and Pt THHs.

MOR		**EGOR**	
Species	Band center/ cm^{-1}	Species	Band center/cm^{-1}
CO_L	1984, 1995 [18, 19]	CO_L	2018, 2025 [18, 19]
CO_B	1842 [18, 19]	CO_B	1857 [18, 19]
CO_M	1794 [6, 20]	CO_M	1827 [6, 20]
$HCOO^-$	1580, 1381, 1351, 1318 [19, 21]	glycolate,	1580, 1410, 1326, 1234, 1075 [17, 22, 23]
CO_3^{2-}	1381 [18, 24]	CO_3^{2-}	1381 [23, 24]
HCO_3^-	1357 [18, 24]	$C_2O_4^{2-}$	1308 [22, 25]
CH_3OH	1016 [26]	HCO_3^-	1357 [6, 22]
		CO_2	2343 [22, 23]

Supplementary References

1. Y. J. Deng, N. Tian, Z. Y. Zhou, R. Huang, Z. L. Liu, J. Xiao and S. G. Sun, *Chem Sci*, 2012, **3**, 1157-1161.
2. Y. Y. Li, H. G. Liao, L. Rao, Y. X. Jiang, R. Huang, B. W. Zhang, C. L. He, N. Tian and S. G. Sun, *Electrochim Acta*, 2014, **140**, 345-351.
3. N. Tian, Z. Y. Zhou, N. F. Yu, L. Y. Wang and S. G. Sun, *J Am Chem Soc*, 2010, **132**, 7580
4. N. Zhang, L. Bu, S. Guo, J. Guo and X. Huang, *Nano Lett*, 2016, **16**, 5037-5043.
5. L. Bu, S. Guo, X. Zhang, X. Shen, D. Su, G. Lu, X. Zhu, J. Yao, J. Guo and X. Huang, *Nat Commun*, 2016, **7**, 11850.
6. Q.-S. Chen, S.-G. Sun, Z.-Y. Zhou, Y.-X. Chen and S.-B. Deng, *Phys Chem Chem Phys*, 2008, **10**, 3645-3654.
7. J. N. Zheng, L. L. He, F. Y. Chen, A. J. Wang, M. W. Xue and J. J. Feng, *J Mater Chem A*, 2014, **2**, 12899-12906.
8. B. A. Kakade, T. Tamaki, H. Ohashi and T. Yamaguchi, *J Phys Chem C*, 2012, **116**, 7464-7470.
9. Y. Liu, M. F. Chi, V. Mazumder, K. L. More, S. Soled, J. D. Henao and S. H. Sun, *Chem Mater*, 2011, **23**, 4199-4203.
10. A. X. Yin, X. Q. Min, Y. W. Zhang and C. H. Yan, *J Am Chem Soc*, 2011, **133**, 3816-3819.
11. S. M. Alia, G. Zhang, D. Kisailus, D. S. Li, S. Gu, K. Jensen and Y. S. Yan, *Adv Funct Mater*, 2010, **20**, 3742-3746.
12. W. Hong, C. S. Shang, J. Wang and E. K. Wang, *Energ Environ Sci*, 2015, **8**, 2910-2915.
13. S. P. Li, J. P. Lai, R. Luque and G. B. Xu, *Energ Environ Sci*, 2016, **9**, 3097-3102.
14. J. J. Lv, L. P. Mei, X. X. Weng, A. J. Wang, L. L. Chen, X. F. Liu and J. J. Feng, *Nanoscale*, 2015, **7**, 5699-5705.
15. P. Song, L. Liu, A. J. Wang, X. Zhang, S. Y. Zhou and J. J. Feng, *Electrochim Acta*, 2015, **164**, 323-329.
16. L. Liu, X. X. Lin, S. Y. Zou, A. J. Wang, J. R. Chen and J. J. Feng, *Electrochim Acta*, 2016, **187**, 576-583.
17. A. Falase, M. Main, K. Garcia, A. Serov, C. Lau and P. Atanassov, *Electrochim Acta*, 2012, **66**, 295-301.
18. Y. Y. Yang, J. Ren, H. X. Zhang, Z. Y. Zhou, S. G. Sun and W. B. Cai, *Langmuir*, 2013, **29**, 1709-1716.
19. Y. M. Zhu, H. Uchida, T. Yajima and M. Watanabe, *Langmuir*, 2001, **17**, 146-154.
20. Q.-S. Chen, A. Berna, V. Climent, S.-G. Sun and J. M. Feliu, *Physical Chemistry Chemical Physics*, 2010, **12**, 11407-11416.
21. Z. Y. Zhou, N. Tian, Y. J. Chen, S. P. Chen and S. G. Sun, *J Electroanal Chem*, 2004, **573**, 111-119.
22. H. Wang, B. Jiang, T. T. Zhao, K. Jiang, Y. Y. Yang, J. W. Zhang, Z. X. Xie and W. B. Cai, *Acs Catal*, 2017, **7**, 2033-2041.
23. L. Demarconnay, S. Brimaud, C. Coutanceau and J. M. Leger, *J Electroanal Chem*, 2007, **601**, 169-180.
24. K. Arihara, F. Kitamura, T. Ohsaka and K. Tokuda, *J Electroanal Chem*, 2001, **510**, 128-135.
25. A. Berna, J. M. Delgado, J. M. Orts, A. Rodes and J. M. Feliu, *Langmuir*, 2006, **22**, 7192-7202.
26. J.-T. Li, Q.-S. Chen and S.-G. Sun, *Electrochim Acta*, 2007, **52**, 5725-5732.